Initial Observations of Starlink Satellites Using the Westford Radio Telescope

Frank D. Lind¹, Samuel Thé¹, Daniel Sheen², Aleks Pop Stefania¹, Ganesh Rajagopalan¹, Mike Poirier¹

¹Haystack Observatory, Massachusetts Institute of Technology, Westford MA, 01886 USA ²Department of Electrical and Computer Science, Massachusetts Institute of Technology, Cambridge MA, 02139 USA

email: {flind,samthe,dsheen,alekspop,ganesanr,mpoirier}@mit.edu

Abstract—We discuss a set of experiments using the Westford radio telescope. These experiments are intended to observe intentional and unintentional radio emissions from mega-constellation satellites such as Starlink. An overview of telescope capabilities is provided that includes details of the feed and receivers used for the observations. Predictions of overflights are used to quantify the visibility of Starlink constellation satellites in azimuth and elevation relative to the Westford telescope location. Combination of the Westford beam pattern with overflight predictions shows that the occurrence rate of satellites in the telescope main beam and sidelobes is already frequent for the current Starlink satellites in orbit. Initial data are presented for a set of experiments where the Westford system was pointed to allow a given Starlink satellite to pass through the beam, where the antenna was scanned in azimuth at a low elevation angle, and where a TLE was used to follow a specific Starlink satellite. We show that in-band emissions from Starlink satellites are detectable at high signal to noise ratios in the main beam. We discuss how observations to date show relatively complex signatures which may depend on the specific satellite, satellite operational state, and the relative satellite to telescope orientation.

Index Terms—astronomy, spectrum, radio interference, Starlink, coexistence

I. INTRODUCTION

Increasing numbers of satellites in low earth orbit (LEO) have resulted in a large number of man made objects carrying radio transmitters and emitting signals that can be detected by ground based radio telescopes. Signals from satellites may include communications transmissions, telemetry, and other signals or emissions that are not intentionally radiated. LEO satellite orbits are generally visible for thousands of kilometers from a receiver site. Signals from satellites can enter the main beam of a telescope or via sidelobes with varying signal strength. Satellites may also reflect signals from ground or space based transmitters when the relative geometries are correct. The signals emitted from mega-constellations such as Starlink are of particular interest due to recent ongoing and rapid increases in the number of operational satellites [1], [2].

If growth in the LEO satellite population continues at its current high rate the frequency with which satellites cross through the primary beam or sidelobes of any given ground based radio telescope will increase dramatically. Collection of quantitative data related to emissions from current and planned mega-constellations is thus vital for understanding and modelling the potential impacts on astronomical systems.

The signals from LEO satellites can act as interference when detected by radio telescopes. Such telescopes are often wideband systems with cryogenic amplifiers that optimize for sensitivity through very low receiver noise temperatures. Sensitive receivers are critical for astronomical measurements but can be susceptible to compression or even damage from strong signals. Radio Frequency Interference (RFI) which enters the telescope generally results in data being discarded in time and frequency. This is only possible when the interference can be detected successfully via characteristics of the signal or by departure from expected data characteristics such as Gaussian signal statistics. Strong signals have the potential to create non-linear responses in radio telescope receiver electronics that can be impossible to remove easily. Such compression can compromise the use of frequencies outside those of the interfering signal. Interference at low signal to noise ratios can also be problematic if it becomes difficult to detect or has noise like characteristics.

Recent observations at low frequencies have quantified unexpected out of band emissions by Starlink satellites. Absolute characterization of such signals over a wide frequency range that includes fundamental signals and any potential harmonics is thus of current interest [2], [3]. These observations are worrying in that out-of-band emissions from LEO satellites will be highly dependent on spacecraft bus designs, specific system hardware components, and satellite operational state. While such emissions may be regulated under various Electromagnetic Compatibility (EMC) standards (e.g. FCC part 15, EMC Directive, 2004/108/EC) reduction below levels detectable by radio telescopes may not be achieved by conformance to currently applicable EMC standards.

Observations using the Westford Radio telescope show that Starlink signals can be clearly detected in expected transmission bands at a high signal to noise ratios. Investigations are underway to quantify in-band and out-of-band emissions over the range of 2 to 14 GHz in terms of calibrated absolute flux. Our early observations have not yet been calibrated.

Efforts are ongoing to calibrate our data and collect a sufficient body of measurements to enable characterization of the signals observable from LEO satellites in the Starlink constellation. Measurements made using the Westford system will also be of use in quantifying the RFI impact of other sources such as Geostationary satellites or emissions from terrestrial systems.

II. THE WESTFORD RADIO TELESCOPE

The Westford Radio Telescope is an 18.3 meter antenna system capable of operating in either a prime focus or Cassegrain configuration. The antenna system has multiple available feeds and is primarily used as a research and development testbed for Geodedic very long baseline interferometry (VLBI) signal chains and receivers [4]. Configuration of the system to act as a smallsat ground station is also possible using UHF for transmission and reception of commands and providing receive only data downlink at S-band or X-band.

A. Feed and Performance

The primary feed on the Westford telescope is an ultrawideband QRFH feed [5] which covers 2 to 19 GHz using a cryogenic dewar and LNA system. System temperatures are generally well below 120K over 2 to 14 GHz with an optimum of less than 60K between 4 and 10 GHz. RF signals from the feed horizontal and vertical polarization channels are brought to the control room for digitization using RF over fiber converters. These converters currently limit the upper frequency coverage to 14 GHz and are also the point at which dynamic range in the system is most limited. The telescope is of a size relevant to current and future radio astronomy systems such as ngVLA [6], [7] if somewhat less sensitive and covering a more limited frequency range. Use of Westford as a testbed for phased array feeds capable of RFI nulling is also currently planned. Operation over a wider frequency range should be possible with such feeds (i.e. up to perhaps 26 to 30 GHz). Ultimately performance is limited at higher frequencies by a combination of the inflated radome that protects the antenna, the overall quality of the antenna surface, and water vapor in the local environment.

B. Receiver configuration

RF to fiber converters are followed by RF updownconverters (UDC) which allow selection of a passband from the antenna in dual orthogonal polarizations (i.e. Hpol and V-pol). Different UDC units are available with 500 MHz and 1 GHz pass bandwidths. The frequency converters provide filtering, gain control, and are frequency locked to the site H-maser standard. A set of very high dynamic range converters capable of 100 MHz to 18 GHz operation are also in integration and will be used in future experiments. Four channels of these converters will be available which will enable simultaneous observations on several frequencies or separation of local RFI using reference antennas. In many cases a dual frequency capability will be used to provide a Starlink telemetry channel as a reference for satellite detection. This can be used to ensure that a satellite is in the beam while observing simultaneously for detection of out of band emissions.

For our initial experiments, Ettus radios have been used including the X300 and N310. We expect to move to the RFSoC 4x2 software radio in future experiments. This will allow us to exploit the full bandwidth of the available downconverters. The use of Ettus radios limits the recording bandwidths possible to date to 125 MHz maximum with half that being stable for longer data acquisition intervals. The Ettus radios provide high dynamic range with additional filtering and gain control. The software radios used are also locked to the site H-maser frequency standard and aligned to the global epoch via PPS triggering of data acquisition. Using Ettus radios, experiments often use a single polarization to maximize bandwidth.

III. OVERFLIGHT PREDICTIONS

For experiment planning, overflights of Starlink satellites are predicted using the full set of TLEs from the constellation and an SGP4 based prediction algorithm [8]. The resulting set of visible passes for each satellite in the constellation are used to compute a table of overflights from which observations can be selected. Generally the rate of satellites in a suitable elevation interval and range from the telescope results in a satellite transiting an observable position once every ten seconds or so for angles above 40 degrees elevation. Many more satellites are potentially visible at lower elevation angles with one every few seconds above 5 degrees elevation. The available number of passes to observe already greatly exceeds our ability to task the telescope for observations.

The aggregate impact of the satellites in the Starlink constellation is also of interest. Figure 1 shows the number of satellites at a given Signal-to-Noise Ratio (SNR) potentially visible to the Westford telescope over a week long interval from 2023-12-04 to 2023-12-11. The telescope is assumed to be pointed at 40 deg elevation and the number of events at a given SNR are shown as a function of azimuth angle. The left-hand side of the figure accounts only for satellites passing through sidelobes of the antenna, whereas the right-hand side only counts the number of satellites transiting through the boresight of the antenna. Figure 2 presents a slice of Figure 1 counting the number of satellites at a given SNR passing through sidelobes of the antenna when it is set to $40 \deg$ elevation and a $180 \deg$ azimuth angle.

Each visible satellite has been assumed to transmit 40 watts of power with a main-lobe gain of 44 dB as an approximation of the actual satellite operating power. Sidelobe levels may be significantly lower (e.g. -38 dB) [1] in practice. Using the main lobe is effectively an upper bound on typical SNR from the constellation.

Accounting for the range of each satellite, the gain pattern of the antenna, the aperture efficiency and the polarization mismatch, attenuation along the path has been estimated. For simplicity, we assume a uniform receive antenna temperature of 125K as a somewhat conservative upper bound. This is based on a model of the antenna, radome, atmosphere, and LNA performance.

Combining the transmit and receive characteristics of the RF paths allows us to estimate the resulting SNR for each

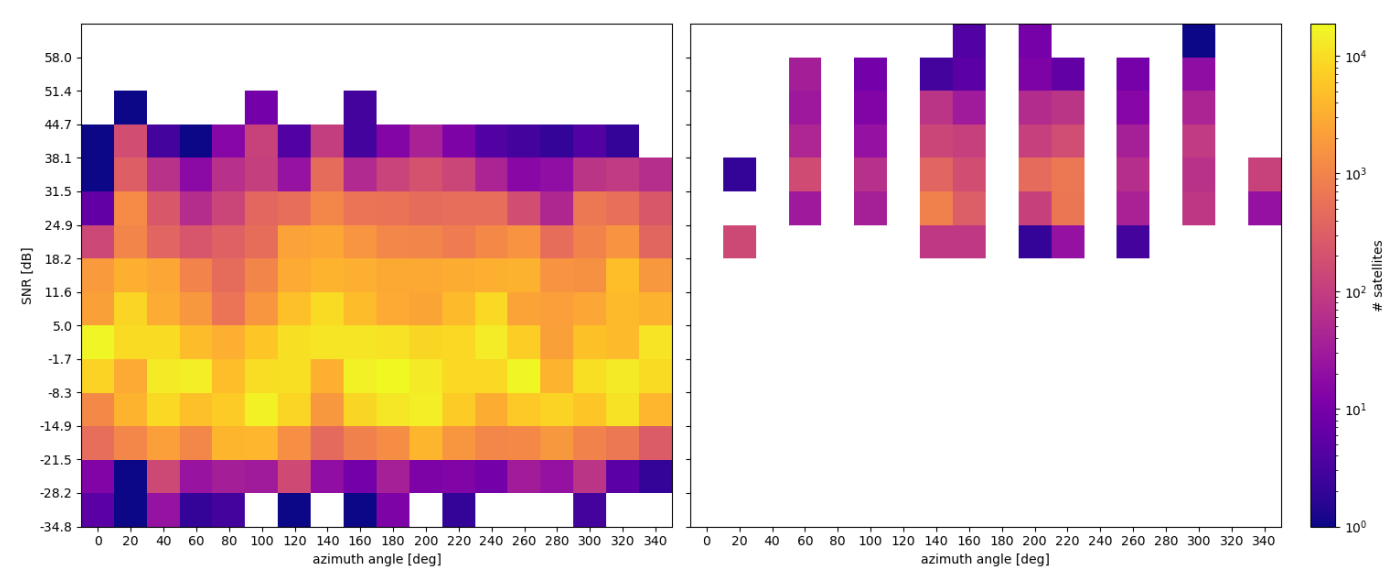


Fig. 1: Modeled number of Starlink satellites at a given SNR potentially observable by the Westford telescope through the antenna sidelobes (left-hand side) and through the mainlobe (right-hand side). Events cover a week from 2023-12-04 to 2023-12-11, at $40 \deg$ elevation and are separated in azimuth angle.

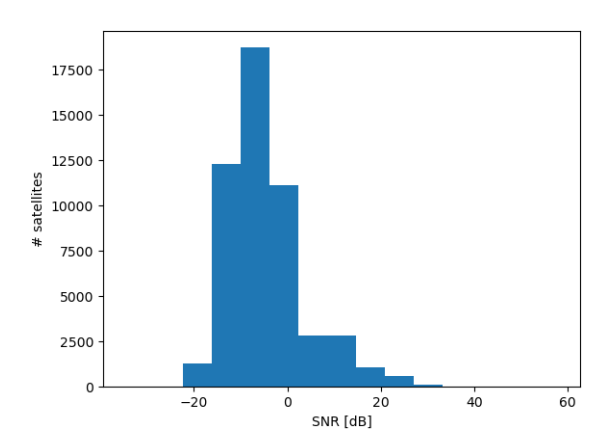


Fig. 2: Modeled number of satellites over a week as a function of their expected SNR at 40 deg elevation and pointing towards 180 deg azimuth (i.e. a slice of Figure 1).

visible satellite. A circular field of view of 90 deg in azimuth was assumed to count the number of satellites possibly visible by the telescope's sidelobes (left-hand side of Figures 1 and 2), where 5 deg from the boresight was masked to reject the satellites passing directly through the center of the beam of the antenna.

A significant number of signals from Starlink satellites are visible at the Westford radio telescope over a week period at an elevation angle of 40 degrees. This is in many ways the worst case for the current constellation population. Distribution in azimuth is relatively uniform with some dependence on the specific orbital geometries present in the constellation. High SNR events are relatively sparse for the time interval under consideration, but are produced by both sidelobes and mainlobe contributions. A significant population of signals

passing through the sidelobes is predicted to exist with low or negative SNR. This distribution shows that sidelobes contributions of LEO RFI sources need to be considered when observing astronomical objects. Indeed, this population will prove difficult to detect but provides a general background of noise that could potentially impact astronomical observations. Observations requiring longer integration in time may be particularly sensitive to this sub-unity SNR population. These distributions are likely to evolve with time as additional satellites are launched and become operational. The occurrence rates are likely to to increase in a manner proportional to overall constellation size.

IV. EXPERIMENTAL OBSERVATIONS

A. Calibration

Calibration of our data acquisition system combines measurement of external calibration sources such as CasA and the Sun with off source measurements to enable SEFD estimation and passband correction. Ultimately quantification of the Westford telescope sensitivity becomes the lower limit for our ability to detect weak signatures from LEO satellites.

As part of our efforts we are developing a comprehensive data driven model of telescope calibration, beam patterns, and performance versus frequency and orientation. Electromagnetic modelling of the Westford antenna pattern is ongoing using a combination of TICRA GRASP, CST microwave, and Feko. Effects of the Westford radome material (i.e. Raydel R60) have also been calculated and compared to measurements.

During operations both a noise calibrator and phase comb generator are available for use via an injection system early in the RF path. These calibrators enable passband monitoring

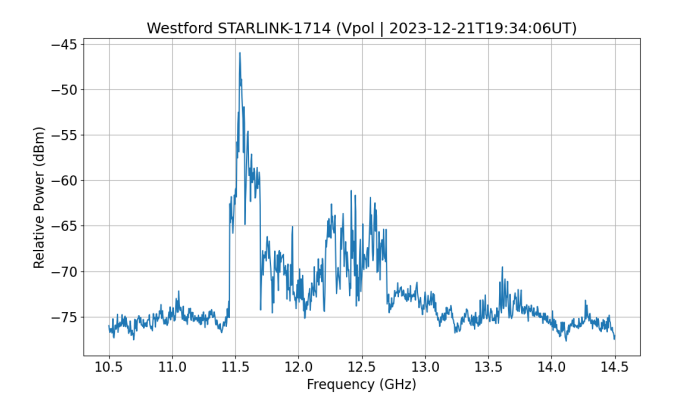


Fig. 3: A wideband Starlink satellite signature captured using a Keysight N9020A spectrum analyzer in peak hold mode.

and correction and can act as a phase reference for the receive chain.

B. Starlink Downlink Observations

Westford observations of Starlink are made using the QRFH feed and software radios with several radios and spectrum analyzers simultaneously connected. Data captures are made using a wideband spectrum analyzer as shown in Figure 3 and as raw data collects of IQ samples. For IQ data the Digital RF data format [9] is used for recording. Typical RF bandwidths collected to date limits recording to at most half of a typical Starlink downlink channel bandwidth [10]. We expect to upgrade to an RFSoC radio and high performance recording system shortly which will enable capture of up to 1 GHz of RF bandwidth at high dynamic range.

During our observations we have attempted three primary methods of Starlink measurement. The first is to predict overflights of individual satellites and select a measurement position at moderately high elevation angles to help exclude terrestrial RFI (i.e. greater than 40 degrees). The satellite is then allowed to transit through the beam and data are recorded for the associated interval. Example data from this approach are shown in Figure 4 where Starlink signatures are clearly visible on several center frequencies. Strong signatures are visible from the satellite transit through the primary beam with sidelobe contributions visible at a later time.

We have attempted a second method where we have scanned the antenna at low elevation angle (e.g. 10 degrees) over its full range in azimuth. Data are then recorded for the entire observation interval. This approach attempts to capture signatures from satellites that intersect the moving beam for a short time interval. Local RFI is often limited in azimuth extent and repeatable between scans. Azimuth scanning observations to date have been done at a rate of 3 degrees per second under computer control. This approach has been successful at detecting terrestrial and geostationary RFI sources but has shown a low probability of intersecting a Starlink satellite and detecting downlink transmissions.

A third approach implemented is to direct the antenna pointing using individual satellite orbital predictions. This form of

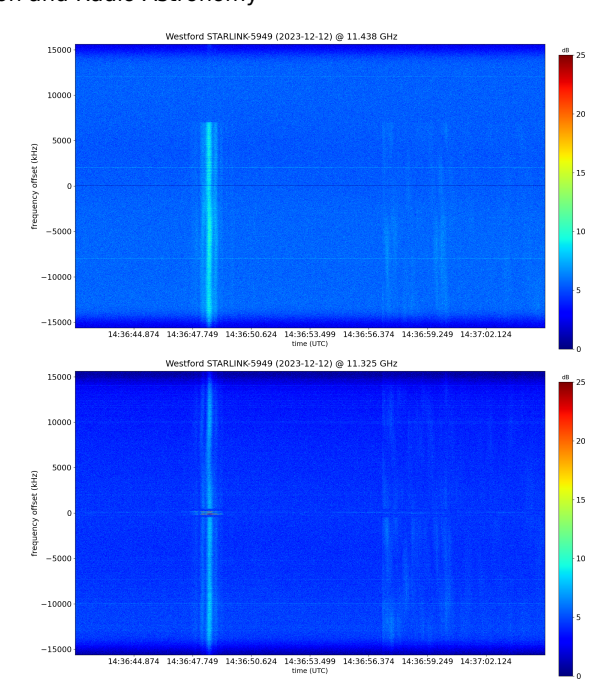


Fig. 4: Observations of STARLINK-5949 as time-frequency spectrograms simultaneously acquired on two frequencies.

directed tracking has been successful using Westford at S-band but is challenging at Ku-band. Currently, only slowly moving passes at low elevation angle can be successfully attempted. This approach has not been very successful to date likely due to the high motion accuracy necessary to dynamically position the satellite in the beam without feedback. A motion control upgrade is ongoing which will improve this capability for future experiments. Directed following of Starlink satellite orbits has the advantage of allowing for longer tracks and a distinctive Doppler shifting of signals over a pass. This may help to separate detected signatures from other potential RFI sources and satellites.

C. Non Starlink Signals

Not all observed signals in our data are from Starlink. For example, Figure 5 shows an observation with the telescope scanning at low elevation angle in vertical polarization. The limited bandwidth only captures a portion of the signal as the beam moves across the satellite's location. In this case the source is most likely a geostationary satellite as the location of the transmission is relatively stable and near the expected elevation and azimuth of a number of known geostationary satellites. The exact satellite generating the signal has not yet been identified.

D. Narrow Leakage Carriers

The frequency intervals in the center of Starlink channels and between downlink bands have been shown to contain narrow carriers [10]. Figure 6 shows a high resolution spectrogram of the signals in this "gutter" interval. Nine separate narrow carriers are visible in a comb like structure in this

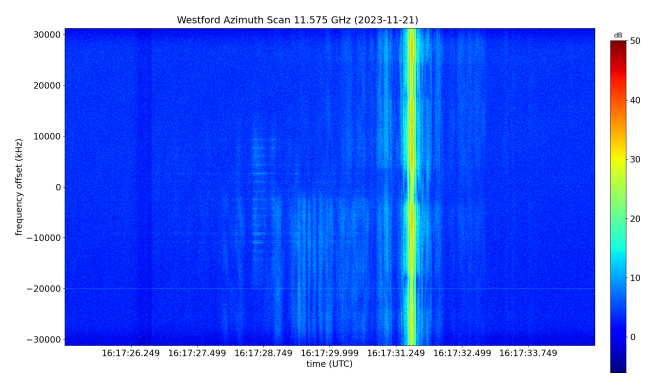


Fig. 5: A time frequency spectrogram of the 12.2 GHz band capturing a very strong geostationary satellite transmission.

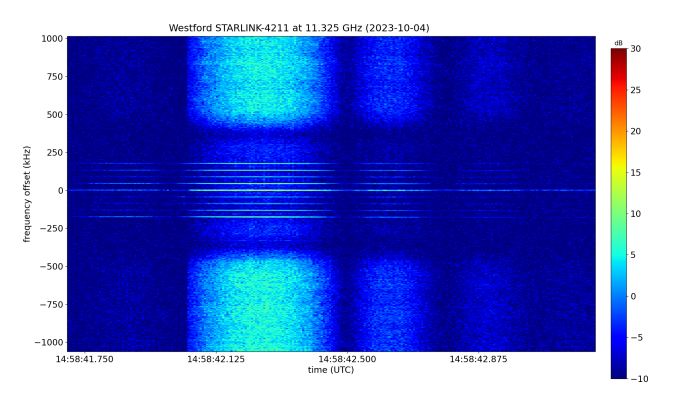


Fig. 6: A signal from STARLINK-4211 is shown as a high resolution spectrogram to highlight leakage carriers in the midchannel gutter.

observation. These carriers generally have higher signal to noise ratio than the corresponding data bands and are detected in advance and after the data downlink signals.

Leakage structures between Starlink channels are not uniformly present in all observations. For example, Figure 7 shows an interval without a comb structure in the top panel while a separate observation of a different satellite shows a distinct comb structure despite having a lower signal to noise ratio for the data channel signals. Comb structure differences between satellites are consistent with prior observations, however the data we present has a higher number of individual tones when compared to the signal structures previously reported [10].

The leakage carrier structures are particularly useful for identification of Starlink satellites due to the distinctive structure they exhibit and generally higher SNR. This may be of value for automating detection of Starlink transmissions.

E. Long Duration Drift Scans

Observations of Starlink satellites drifting through the beam results in detection of a range of signal levels. Particularly strong signals are likely due to detection of Starlink transmissions where the satellite is oriented in the general direction of Westford. It seems likely that the variability observed may also be due to differences in activity generated by user ground

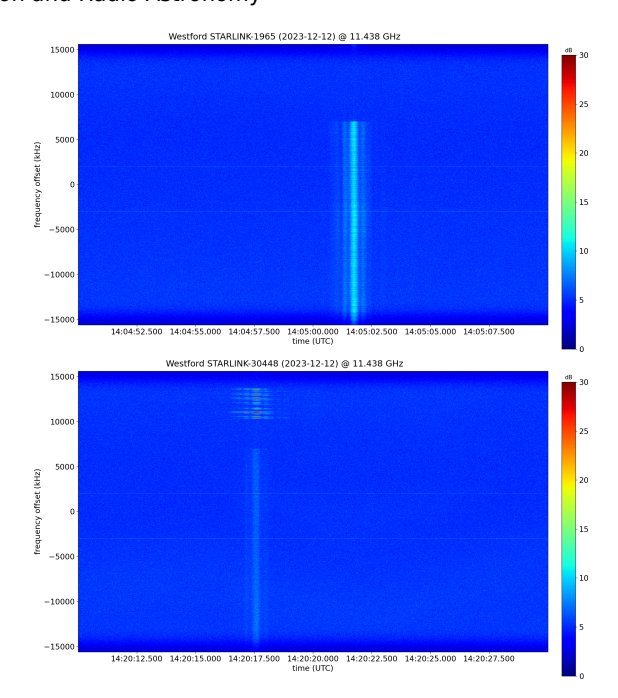


Fig. 7: Observations at separate times of the same frequency range for two different Starlink satellites with only one showing a comb structure between channels.

terminals. The time behavior could also reflect aspects of the transmission geometry or propagation path which are dynamic and for which we have not yet accounted.

Signals detected during long duration drift scans have shown significant variations at low signal to noise ratios. This may be due to the superposition of signals from one or more satellites visible within antenna pattern sidelobe structure. Additional experiments focused on validating our statistical modelling of the Starlink satellite population are planned.

V. DISCUSSION

A moderate fraction of our observations to date have strong downlink signatures from Starlink satellites. Observations which dwell at a specific expected location and wait for satellite transit have proven to be the most successful. Repeated observations of the same satellite shows that signal levels vary significantly from one observation interval to another.

In all cases only a sub-set of all available downlink data channels are active. There seems to be some consistency in the activated channels from satellite to satellite. This may reflect a regional mode of operation or interaction of the satellites with the ground terminal network which exists in the New England region. At their very strongest the Starlink signals can compress the existing Westford receiver chain. This remains relatively infrequent but our sampling to date is biased somewhat based on filtering of satellites for moderate elevation angles and larger overall distances. It should be noted that other signals outside the Starlink bands compress the Westford receivers much more frequently. Noise floor variations due to

compression are easily visible in spectrum analyzer monitoring and recorded IQ data when they occur.

Separation of Starlink and non-Starlink signals in scanning experiments has proven very challenging despite some evidence of generally persistent interference at low signal to noise ratios. Some of the signals detected are very similar in frequency and nature to the Starlink transmissions with notable differences in the detailed transmission channel structures.

Observations during directed following of Starlink TLE predictions have also been less successful than expected. This is likely due to limitations in the motion controller that is currently used to point the Westford antenna system. We expect the motion control improvements currently underway to improve this performance in the near future.

Wideband monitoring using a spectrum analyzer has been vital for consistent detection of satellites. It also provides a clear indication of Starlink channel structure. In some cases the duration of the detection is such that we clearly see a trace of the Starlink antenna pattern in the Westford main beam (i.e. the Westford beam is very narrow, less than 0.1 degree at 12 GHz). Other cases show much weaker signatures that are likely associated with sidelobes and a combination of the Westford and satellite antenna patterns. Some observations show only short transient signatures which can be difficult to definitively attribute to the satellite under observation.

Narrow band drift scan experiments in the Starlink 11.325 GHz mid-channel gutter show a low level of weak background signals consistent with more distant satellites contributing energy to the overall band noise floor. There appears to be significant structural variation in this floor in time and frequency. In some cases this may be due to strong signals impinging on the telescope antenna pattern sidelobe structure. These weak signatures can be difficult to detect with the limited integration times available as the satellites in the constellation move and evolve through the Westford antenna pattern. Work to characterize and model the combined effect of the Starlink constellation on the overall noise background needs to be undertaken.

Future efforts using Westford will include development of a more precise calibration model, observation of Starlink satellites systematically in and out of band (i.e. from 2 to 14 GHz), and additional directed following of individual Starlink satellites in their orbits. This later tracking of Starlink satellites based on TLE predictions with receivers capable of large bandwidths will ultimately provide the definitive data needed for both in-band and out-of-band characterization. Separation of different satellite and terrestrial RFI signals can be challenging and care must be taken in interpreting collected data. For example, geostationary satellite downlinks are highly visible to Westford in specific directions and look superficially similar to Starlink transmissions. These could easily be confused with Starlink signals in a monitoring system having insufficient spatial resolution or when unexpectedly pointing at more than one satellite simultaneously. This may become an increasing issue as multiple satellite constellations overlap in different altitude ranges.

We ultimately hope to quantify in and out of band emissions in terms of absolute flux. This information will enable development of an empirical model that allows for prediction of the signal levels observable by Westford or any similar radio telescope. Such a model may be useful for evaluating the impact of Starlink or similar mega-constellations as the overall constellation sizes grow. Extension of the model to additional satellite types will also be possible by characterization of the specific signals from a given class of satellites. Incorporation of different radio telescope characteristics and antenna patterns will also be necessary.

Future mega-constellations are of particular concern due to the rapid growth of these systems and the difficulty inherent in avoiding, detecting, and removing their signals from astronomical observations. Both in-band and out-of-band emissions need to be measured and used as the basis for quantitative empirical modelling of potential interference. Such modelling may become necessary for any set of collected astronomical observations to aid in the separation of interference from the astronomical signals of interest.

ACKNOWLEDGMENTS

We would like to thank the Westford team including A. Burns, T. Bettencourt, C. McKenney, and C. Eckert for their contributions to the construction, installation, testing, and experimental use of the Westford telescope, feeds, and receiver systems. Additionally, we acknowledge the support of the National Science Foundation under awards SII-2029670 and AST-2132700.

REFERENCES

- [1] C. De Pree, U. Rau, R. Selina, B. Svoboda, and A. Beasley, "Evla memo no. 223," 2023.
- [2] F. Di Vruno, B. Winkel, C. Bassa, G. Józsa, M. Brentjens, A. Jessner, and S. Garrington, "Unintended electromagnetic radiation from starlink satellites detected with lofar between 110 and 188 mhz," Astronomy & Astrophysics, vol. 676, p. A75, 2023.
- [3] D. Grigg, S. Tingay, M. Sokolowski, R. Wayth, B. Indermuehle, and S. Prabu, "Detection of intended and unintended emissions from starlink satellites in the ska-low frequency range, at the ska-low site, with an ska-low station analogue," *Astronomy & Astrophysics*, vol. 678, p. L6, 2023.
- [4] C. Beaudoin, K. Wilson, B. Whittier, A. Whitney, R. McWhirter, J. SooHoo, D. Smythe, C. Ruszczyk, A. Rogers, M. Poirier *et al.*, "Vlbi2010 and the westford station—the path forward," *Proceedings*, p, vol. 52, p. 56, 2012.
- [5] A. Akgiray and S. Weinreb, "Ultrawideband square and circular quadridge horns with near-constant beamwidth," in 2012 IEEE International Conference on Ultra-Wideband. IEEE, 2012, pp. 518–522.
- [6] M. McKinnon, A. Beasley, E. Murphy, R. Selina, R. Farnsworth, and A. Walter, "ngvla: The next generation very large array," *Bulletin of the American Astronomical Society*, vol. 51, no. 7, p. 81, 2019.
- [7] R. Selina and E. Murphy, "ngvla reference design development & performance estimates," ngVLA Memo# 17, vol. 18, 2017.
- [8] D. Vallado and P. Crawford, "Sgp4 orbit determination," in AIAA/AAS Astrodynamics Specialist Conference and Exhibit, 2008, p. 6770.
- [9] R. Volz, W. C. Rideout, J. Swoboda, J. P. Vierinen, and F. D. Lind, "Digital rf." [Online]. Available: https://github.com/MITHaystack/digital_rf
- [10] T. E. Humphreys, P. A. Iannucci, Z. M. Komodromos, and A. M. Graff, "Signal structure of the starlink ku-band downlink," *IEEE Transactions on Aerospace and Electronic Systems*, 2023.